Transport Diffusivities of CH_4, CF_4, He, Ne, Ar, Xe, and SF_6 in Silicalite from Atomistic Simulations

Anastasios I. Skoulidas and David S. Sholl*

Department of Chemical Engineering, Carnegie Mellon University, Pittsburgh, Pennsylvania 15213

Received: November 20, 2001; In Final Form: March 19, 2002

We have used atomistic simulations to examine the adsorption isotherms, self diffusivity, and transport diffusivity of seven light gases, CH_4, CF_4, He, Ne, Ar, Xe, and SF_6, adsorbed as single-components in silicalite at room temperature. By using equilibrium molecular dynamics, the self and transport diffusivities are computed simultaneously. For each species the self diffusivity decreases as pore loading is increased due to steric hindrance from other adsorbed molecules. In contrast, the transport diffusivity is an increasing function of pore loading for each species. Our results are the most extensive collection of transport diffusivities determined from atomistic modeling of adsorption in a zeolite to date, and they allow us to examine the accuracy of several common approximations to the loading-dependent diffusivities. Carefully converged results for the anisotropy of diffusion of CH_4, CF_4, He, Ne, Ar, Xe, and SF_6 in silicalite are presented. We discuss the implications of our results for understanding self and transport diffusivities in mesoporous materials and for multi-component mixtures in microporous materials.

I. Introduction

Diffusion of molecules adsorbed in the pores of zeolites is a central feature of the many industrial processes that utilize zeolites for separations and catalysis.[1−4] Despite extensive research, even the apparently simple case of a single adsorbed species diffusing in a defect-free zeolite crystal as a function of the adsorbate concentration is still not completely understood. The diffusion of a single adsorbed species can be characterized by two distinct diffusivities.[1−5] The *self diffusivity* at a specified concentration, $D_s(c)$, measures the displacement of a tagged molecule as it diffuses at equilibrium inside a crystal where the total adsorbate concentration is c. The self diffusivity is conveniently defined using the Einstein expression

$$D_s(c) = \lim_{t\to\infty} \frac{1}{6t}\langle|\vec{r}(t) - \vec{r}(0)|^2\rangle \tag{1}$$

or, equivalently, in terms of the velocity autocorrelation function of the tagged particle,

$$D_s(c) = \frac{1}{3}\int_0^\infty \langle\vec{v}(0)\,\vec{v}(t)\rangle\,dt \tag{2}$$

Here, $\vec{r}(t)$ and $\vec{v}(t)$ are the position and velocity of the tagged particle, respectively. These two expressions have been written in a form appropriate for an isotropic three-dimensional pore structure, but can easily be generalized to anisotropic materials.[2,3]

Macroscopic diffusion of a single adsorbed species in a zeolite can be characterized by using the *transport diffusivity*, $D_t(c)$, which is defined as the proportionality constant relating a macroscopic flux, $\vec{J}$, to a macroscopic concentration gradient:

$$\vec{J} = -D_t(c)\nabla c \tag{3}$$

Again, this expression is suitable for an isotropic medium but can be easily generalized to anisotropic materials. Recognizing that the chemical potential is a more appropriate driving force for diffusion than simply concentration, the transport diffusivity is often rewritten as

$$D_t(c) = D_0(c)\left(\frac{\partial \ln f}{\partial \ln c}\right)_T \tag{4}$$

Here, f is the fugacity of the bulk phase that is at equilibrium with the adsorbed phase when the latter has concentration c, and $D_0(c)$ is called the *corrected diffusivity*.[2,3] The term involving the logarithmic derivative of the fugacity is referred to as the thermodynamic correction factor and can be evaluated provided the equilibrium adsorption isotherm for the material being studied is known.

We note that each of the three diffusivities defined above have other common names. The self diffusivity is also known as the tracer diffusivity.[6] The transport diffusivity is also referred to as the Fickian diffusivity,[5,7] the chemical diffusivity,[6] or the collective diffusivity.[8] Finally, the corrected diffusivity is also known as the jump diffusivity.[6] For clarity, we will only refer to these quantities as the self, transport, and corrected diffusivities (denoted D_s, D_t, and D_0, respectively) in the remainder of this paper.

Equations 1−4 are written in a form that emphasizes the fact that the self, transport, and corrected diffusivities are in general concentration dependent.[1−3] These three quantities are also in general not equal.[1−3] D_s, D_t, and D_0 are equal only in the limit of vanishing concentration of the adsorbate:

$$D_s(c=0) = D_t(c=0) = D_0(c=0) = D(0) \tag{5}$$

Here we have defined $D(0)$ as the zero loading molecular diffusivity. Since self and transport diffusivities are typically only accessible via different experimental methods, there has been long standing interest in comparing these two diffusivities. Such a comparison has frequently been based on the assumption

* Corresponding author. Fax: 412-268-7139. E-mail: sholl@andrew.cmu.edu.

10.1021/jp014279x CCC: $22.00
Published on Web 04/23/2002

that the corrected diffusivity is independent of the adsorbate concentration. With this approximation, eqs 4 and 5 give

$$D_t(c) \approx D(0)\left(\frac{\partial \ln f}{\partial \ln c}\right)_T \tag{6}$$

This approximate expression is referred to as the Darken approximation, although this name is not historically accurate.[4,9,10] Despite its widespread use, little is known about the accuracy of eq 6. Given the well-known discrepancies between experimental measurements of self and transport diffusivities when these quantities are compared on the basis of eq 6, it is useful to develop a general understanding of when eq 6 is inaccurate. Computer simulations provide a useful avenue for examining the relationships between self, transport, and corrected diffusivities in zeolites because all three quantities can be unambiguously determined under fixed conditions.[2,3,9]

In this paper we restrict our attention to diffusion of small molecules in defect-free silicalite-1 (hereafter simply referred to as silicalite). This material is the siliceous form of ZSM-5 and has been widely studied.[3] We have also recently examined molecular diffusion in other siliceous zeolites to examine the impact of pore shape and size and will report these results elsewhere.[11] It is important to note that there may be important differences between molecular diffusion in silicalite and in its Al-substituted isomorph, ZSM-5.[12,13] Trout et al.[12] and Coppens et al.[13] have studied lattice models of ZSM-5 in which Al-substituted sites were assumed to exhibit stronger binding of adsorbates than nonsubstituted sites. The presence of these strong binding sites can have a dramatic qualitative impact on the concentration dependence of both self and transport diffusivities. Chen, Falcioni, and Deem have also examined models of cationic zeolites and showed that long-range ionic disorder can lead to significant complications in comparing diffusivities measured with experimental methods that examine substantially different time scales.[14]

To set the stage for our results, it is useful to briefly review the results that have been obtained for two different classes of simulations, lattice models and atomistic simulations. Lattice gas (LG) models for molecular diffusion in silicalite have been studied by several groups.[12,13,15,16] The critical assumptions of these models are (1) molecules reside only at discrete sites in the crystal pores, (2) molecules diffuse by hopping between sites in an uncorrelated fashion, (3) the only interactions between adsorbates are steric repulsions that prohibit multiple molecules from occupying the same lattice site, and (4) the adsorption energy of all sites are identical. Assumption (1) means that the adsorbate concentration is conveniently described using the fractional loading, θ, with $0 \leq \theta \leq 1$. Assumption (2) means that the rate at which a molecule attempts to hop away from a site is determined only by the identity of the site, not by the population of nearby molecules or the past history of the molecule attempting to hop. The success of an attempted hop is, of course determined by the presence of nearby molecules, as required by assumption (3). Although lattice models with various collections of lattice sites and anisotropic diffusion rates have been studied,[12,13,15,16] several simple results for the self, corrected, and transport diffusion apply to all these models. The self diffusivity decreases monotonically with loading, obeying

$$D_s^{LG}(\theta)/D(0) = (1 - \theta)\, f(\theta) \tag{7}$$

where $f(\theta)$ is a function accounting for correlation effects.[13,15,16] The detailed form of $f(\theta)$ depends on the lattice topology and hopping anisotropy, but in all cases $f(\theta) \leq 1$. The loading dependence of the corrected and transport diffusivity for these LG models is very simple. The corrected diffusivity decreases linearly with loading,

$$D_0^{LG}(\theta)/D(0) = (1 - \theta) \tag{8}$$

and the transport diffusivity is constant,

$$D_t^{LG}(\theta)/D(0) = 1 \tag{9}$$

The relationship between the corrected and transport diffusivities reflects the fact that the thermodynamic correction factor is simply $1/(1 - \theta)$ for a lattice model in which the adsorption energy of all sites are identical. It is important to note that eq 9, which is exact for the lattice models described above, is qualitatively different from eq 6. In other words, the Darken approximation is qualitatively inaccurate for systems that are well described by the lattice models defined above. We reiterate that the discussion above is restricted to a class of LG models that has been used to model the diffusion of small molecules in silicalite. It is of course possible to consider LG models that do not assume that all adsorption sites have the same energy, that only steric repulsions exist between adsorbates and so on. More complicated dependences of the diffusivities on loading occur for LG models that include energetic interactions between adsorbates or lattice sites with unequal binding energies.[12,13]

There is an extensive body of work that uses atomistic models of molecular adsorption in zeolites to examine diffusion, particularly in noncationic materials such as silicalite.[2,3] Much of this work has focused on self diffusivities, which can be determined from Molecular Dynamics (MD) calculations using eqs 1 or 2. A smaller number of studies have calculated corrected and transport diffusivities from atomistic models.[9,17] Following an initial series of calculations by Maginn et al.[17] we recently calculated the self, corrected, and transport diffusivities of atomistic models of CH_4 and CF_4 in silicalite as functions of concentration and temperature.[9] Both atomistic models give adsorption isotherms that are well approximated by Langmuir isotherms, although more accurate fits are possible using more flexible functions for the isotherms.[9] For both species, the self diffusivity decreases monotonically with increasing concentration, as in eq 7.[9,17−19] It is interesting to note that Paschek and Krishna have derived a LG model for CH_4 and CF_4 in silicalite that matches the orientationally averaged self diffusivity of these species observed in MD simulations at 300 K over a wide range of loading.[20] This LG model is slightly more complicated than the model outlined above in that it has small difference in adsorption energy between several classes of binding sites. It also exhibits a different saturation loading than the atomistic models.[20]

In another paper Paschek and Krishna report the Fickian diffusivity for their LG model of CH_4 as a function of concentration.[16] Their LG model gives results very similar to eqs 8 and 9, as expected. It is useful to compare atomistic realizations of the transport and corrected diffusivities to these simple LG results. For the atomistic model of CH_4 in silicalite, the transport diffusivity increases monotonically with concentration,[9,17] in sharp contrast to eq 9 and the results of Paschek & Krishna.[16] Examination of the corrected diffusivity (see below) shows that eq 6 is quite accurate for the atomistic description of CH_4 in silicalite, except at the highest concentrations. For the atomistic model of CF_4 in silicalite, the transport diffusivity is approximately constant for low pore loadings (<4 molecules/unit cell) but is an increasing function of loading for higher loadings. This behavior is qualitatively different from that

TABLE 1: Lennard-Jones Potential Parameters for CH_4, CF_4, He, Ne, Ar, Xe, and SF_6 in Silicalite

adsorbate	ref	ϵ_{AA} (K)	σ_{AA} (Å)	ϵ_{AZ} (K)	σ_{AZ} (Å)
CH_4	[19]	147.9	3.73	133.3	3.214
CF_4	[21]	134	4.66	109.6	3.73
He	[27]	10.223	2.28	51.235	2.62
Ne	this work	35.7	2.789	56.87	2.798
Ar	[23]	124.07	3.42	95.61	3.17
Xe	[25]	221	4.1	135.87	3.454
$Xe_{(II)}$	[26]	224.992	4.064	201.949	3.296
SF_6	[23]	222.1	5.13	147.21	3.97

predicted by LG models (cf. eq 9). Moreover, the Darken approximation (eq 6) was found to be quite inaccurate for the atomistic model of CF_4 in silicalite.[9]

To summarize the discussion above, LG and atomistic models of CH_4 and CF_4 in silicalite give consistent self diffusivities but inconsistent transport diffusivities. The Darken approximation is inaccurate for the LG models of both species. For the atomistic model of CH_4 in silicalite, the Darken approximation is accurate, but not for CF_4 in silicalite.[9] Since LG models provide only an approximate description of the dynamics of adsorbed molecules, it is important to understand how general the discrepancies between these models and more detailed atomistic models are. Similarly, since the Darken approximation is widely used for describing macroscopic molecular transport in zeolites, it is useful to understand the circumstances under which this approximation is actually valid.

In this paper we describe the single-component self, corrected, and transport diffusivities for atomistic models of 7 small molecules, CH_4, CF_4, He, Ne, Ar, Xe, and SF_6, adsorbed in silicalite. This is the largest set of data for corrected and transport diffusivities reported to date for atomistic simulations of molecular diffusion in zeolites. In Section II, the details of our atomistic models and molecular simulations are described. The self diffusivities of CH_4, CF_4, He, Ne, Ar, Xe, and SF_6 in silicalite are presented in Section III, followed by the transport and corrected diffusivities of these species in Section IV. The implications of our results for predicting the accuracy of eq 6 and for using LG models to describe macroscopic molecular transport in zeolites are discussed in Section V.

II. Details of Model and Calculations

The small molecules studied in this work were all modeled as spherical particles. Adsorbate−adsorbate interactions were modeled using a Lennard-Jones potential. Following standard methods for modeling light gases in noncationic zeolites, the interaction between adsorbed molecules and the zeolite's silicon atoms is not explicitly included. The interaction between adsorbed molecules and the zeolite framework was modeled by using a pairwise Lennard-Jones potential acting between each adsorbate and oxygen atom in the zeolite. The Lennard-Jones potentials have the standard form $U(r) = 4\epsilon[(\sigma/r)^{12} - (\sigma/r)^6]$ where the parameters σ and ϵ are of course different for adsorbate−adsorbate and adsorbate−zeolite interactions. The interaction parameters used in our study are shown in Table 1.

Most of the potential parameters listed in Table 1 were obtained from the literature. We used parameters for CH_4 from Goodbody et al.[19] For this potential, the methane−oxygen interaction energy was adjusted to fit the experimental Henry's law constant for methane adsorbing in silicalite at room temperature. The parameters for CF_4 were obtained from Heuchel et al.[21] This potential uses adsorbate−adsorbate interactions from the literature [22] and adsorbate−zeolite parameters determined using the Lorenz-Berthelot combining rules. SF_6 and Ar parameters were taken from Clark et al.[23] For both of these species the adsorbate−adsorbate parameters were obtained from Reid et al.[22] SF_6−oxygen parameters were derived using the Lorenz-Berthelot rules as for CF_4. The Ar-oxygen parameters were adjusted to fit adsorption experiments at 77 K. We determined potential parameters for Xe and Ne. The Xe and Ne adsorbate−adsorbate interaction parameters were obtained from the literature.[22,24] We determined adsorbate−oxygen parameters using the procedure described in June et al.[25] With this procedure, the Lennard-Jones dispersion (attraction) constant was determined with the Slater−Kirkwood equation, which requires knowledge of the effective number of electrons n_e, and atomic polarizabilities. The repulsion constant was determined from a force balance at the sum of the van der Waals radii for the Xe (Ne)−oxygen pair. For Xe we have also used an additional set of potential parameters derived by Pickett et al.[26] For the rest of the paper we refer to this set of Xe parameters as $Xe_{(II)}$. The parameters for $Xe_{(II)}$ were derived by adjusting them to fit the experimental internal energy of adsorption. He parameters were taken from Chakravarty.[27] For this potential, the adsorbate−adsorbate parameters were taken from the literature[28] while the adsorbate−zeolite parameters were calculated using the same procedure described above for Ne and Xe.

In all of our simulations, silicalite was assumed to be rigid in its orthorhombic (*Pnma*) form. An experimentally determined crystal structure was used[29] with cell parameters $a = 20.07$ Å, $b = 19.92$ Å, and $c = 13.42$ Å. The silicalite lattice contains two types of channels: straight channels along the *y* direction and zigzag channels across the *x* direction. These two types of channels are interconnected creating a three-dimensional network. Previous studies[25,30] have shown that holding the lattice rigid does not significantly affect the dynamics of small molecules in silicalite. Evaluation of the adsorbate−zeolite potentials and forces was performed by precomputing the values of these functions on a grid covering the crystallographic unit cell and subsequently interpolating the function's values from this grid.[17,19,31] We used a grid with resolution 0.2 Å and cubic Hermite polynomial interpolation.[31,32] We tested this approach by computing the Henry's law constant, K_H, for CH_4 in silicalite at 298 K at infinite dilution using the method of Goodbody et al.[19] The difference in K_H between using the interpolated potential and the computationally intensive direct approach was less than 1%.

For all the simulations reported here the cutoff distance for the interactions was set to 13 Å. For the GCMC simulations, long-range corrections for the zeolite−adsorbate interaction were added assuming a uniform oxygen density for distances greater than the cutoff distance. In the MD simulations all the interactions were cut and shifted to ensure continuous forces. A $2 \times 2 \times 2$ unit cell simulation box was used for all the simulations with 4 or more molecules per unit cell. In general, a $3 \times 3 \times 3$ unit cell simulation box was used for concentrations less than 4 molecules per unit cell. For weakly adsorbing species, simulation boxes as large as $10 \times 10 \times 10$ unit cells were used while simulating adsorption isotherms at low and moderate pressures. In all of the simulations reported here the temperature was fixed at 298 K.

We have calculated the adsorption isotherms of each molecule at room temperature using Grand Canonical Monte Carlo (GCMC) simulations.[17,21,33] The chemical potential of each bulk gas was related to its pressure by a virial equation of state. For CH_4 and CF_4, the virial expansion was taken up to the fourth virial coefficient using the coefficients determined experimen-

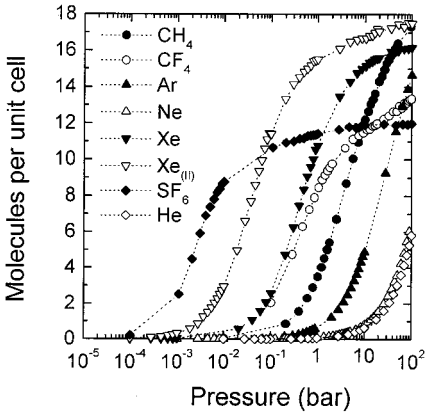

Figure 1. Adsorption isotherms of CH_4 (filled circles), CF_4 (open circles), He (open diamonds), Ne (open up triangles), Ar (filled up triangles), Xe (filled down triangles), $Xe_{(II)}$ (open down triangles), and SF_6 (filled diamonds) in silicalite computed using GCMC.

tally by Doulsin et al.[34] For the rest of the gases, virial coefficients up to the third were obtained from Dymond et al.[35] All GCMC simulations included 4×10^6 single particle Monte Carlo moves for equilibration, followed by 6×10^6 Monte Carlo moves for production. The statistical uncertainties were estimated by dividing the production run into 10 blocks and calculating the standard deviation of the block averages. We verified that the Henry's law constants obtained from fitting the isotherms from our GCMC results are in excellent agreement with those computed independently using the method of Goodbody et al.[19]

The adsorption isotherms for CH_4, CF_4, He, Ne, Ar, Xe, $Xe_{(II)}$, and SF_6 are shown in Figure 1, where we plot the number of adsorbate molecules per unit cell (loading) as a function of the pressure in a log−linear scale. The observed uncertainty for CH_4 at ∼8 and ∼0.5 molecules per unit cell was 0.8% and 1.2%, respectively. Similar uncertainties were observed for all other species. The calculated isotherms for CH_4 and CF_4 agree very well with experiments[21,36] for low to moderate pressures. For higher pressures the adsorption isotherm for CH_4 in Figure 1 slightly underestimates the experimental values, while the CF_4 loading is overestimated relative to experiments.[21,36] The calculated isotherms for Ar slightly overestimate the experimental values at low pressures, while the isosteric heats of adsorption are slightly underestimated.[37] For SF_6 the loading is underestimated relative to experiments at low pressures while the isosteric heats of adsorption are overestimated.[37]

As mentioned above, LG models for adsorption in zeolites are typically discussed in terms of the fractional occupancy of lattice sites. To compare our atomistic results with LG models, it is necessary to define the saturation loading for each species. We feel it is important to emphasize that for atomistic representations of adsorbates, this notion of a saturation loading cannot be absolutely defined. This observation follows from the fact that our adsorbates, as with real molecules, are not hard spheres and can therefore always be compressed when acted on by a sufficient driving force.[38] Many previous studies have assigned saturation loadings to atomistic models by using GCMC to determine an adsorption isotherm over a specific pressure range and fitting the resulting data with a functional form (e.g., a Langmuir isotherm) that yields an effective saturation loading.[17,21] A difficulty with this procedure is that the fitted saturation loading is dependent on the range of fitted data. We have taken a slightly different approach to this issue by noting that as the loading in the zeolite increases, the isosteric heat of adsorption typically drops precipitously and becomes

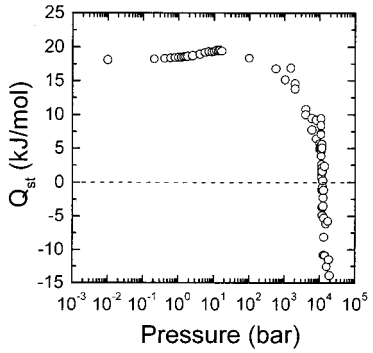

Figure 2. Isosteric heat of adsorption of methane in silicalite at 298 K as a function of pressure.

TABLE 2: Saturation Loading, n_{Sat} (molecules/unit cell), and Zero Loading Diffusivity at 298 K, $D(0)$, for CH_4, CF_4, He, Ne, Ar, Xe, and SF_6 in Silicalite

adsorbate	n_{sat}	$D(0)$ (10^{-4} cm^2 s^{-1})
CH_4	32	1.45
CF_4	16.5	0.451
He	175	6.58
Ne	94	2.74
Ar	35.6	1.32
Xe	20.2	0.404
Xe_{II}	22.5	0.232
SF_6	15.5	0.0532

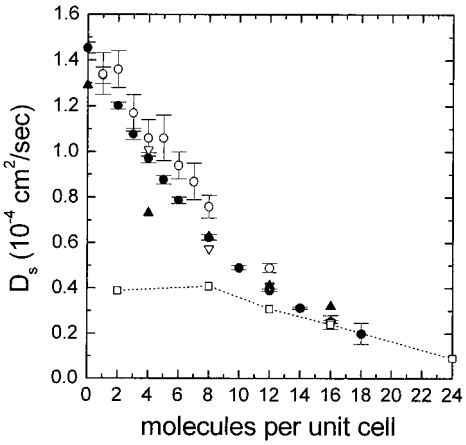

Figure 3. Orientationally averaged self diffusivities of methane in silicalite at 298 K from various authors: ref 9 (filled circles), ref 19 (open circles), ref 41 (open down triangle), ref 25 (filled up triangle), ref 40 (open square).

negative at sufficiently high bulk phase gas pressures. An example of this behavior for CH_4 in silicalite is shown in Figure 2. We computed the isosteric heats from our GCMC simulations using the method described in ref 39. We define the saturation loading, n_{sat}, as the loading where the isosteric heat of adsorption is zero. We have determined the saturation loading of each species we have considered using this criterion. The observed saturation loadings are summarized in Table 2. In what follows we only use these saturation loadings to present our data in a dimensionless form that can be compared with LG models by defining $\theta_i = n_i/n_{i,sat}$. The numerical values of the saturation loadings play no role in our calculations of molecular diffusivities. The main disadvantage of the method we have chosen to define n_{sat} is that it requires considering unphysically high pressures (cf. Figure 4). For the species we have considered, pressures in the range of 9000−14000 bar were required to define n_{sat}, with the exception of He, which required simulating pressures exceeding 20000 bar. We repeat that the saturation

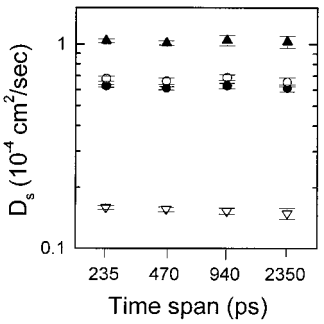

Figure 4. Orientationally averaged self diffusivity (filled circles), and *x* component (open circles), *y* component (filled triangles), and *z* component (open triangles) of self diffusivities of methane in silicalite at room temperature showing the convergence of the calculated averages with increasing size of time spans.

loading cannot be defined absolutely for systems that include nonhard sphere interactions, so this quantity should always be used with caution.

To calculate the self-and corrected diffusivities of adsorbed molecules we have used Equilibrium Molecular Dynamics (EMD) simulations. The simulations were conducted in the canonical ensemble using a Nosé-Hoover thermostat. We checked that we get equivalent results for both diffusivities using NVE-EMD simulations. The self diffusivity can be efficiently calculated from an EMD trajectory using

$$D_s = \lim_{t\to\infty} \frac{1}{6t}\left\langle \frac{1}{N}\sum_{l=1}^{N}\left|\left|\mathbf{r}_l(t) - \mathbf{r}_l(0)\right|\right|^2 \right\rangle \qquad (10)$$

Here, $\langle ... \rangle$ denotes an ensemble average and N is the number of adsorbed molecules in the simulation. As described elsewhere[9] the corrected diffusivity can be calculated from EMD simulations using an efficient method first described by Theodorou et al.[2,17] This method uses an Einstein relationship similar to eq 10 that measures the mean square displacement of the center of mass of the adsorbed molecules:

$$D_0 = \frac{1}{6N}\lim_{t\to\infty} \frac{1}{t}\left\langle \left|\left|\sum_{l=1}^{N}(\mathbf{r}_l(t) - \mathbf{r}_l(0))\right|\right|^2 \right\rangle \qquad (11)$$

Equations 10 and 11 can easily be generalized to determine the *x*, *y*, or *z* component of a diffusivity by replacing the factor of 6 by a factor of 2 and by using the desired component of position instead of the position vectors.[2,19] The orientationally averaged diffusivities shown in eqs 10 and 11 are related to the individual components of the diffusivities by $D = (D_x + D_y + D_z)/3$.

Each MD simulation started with the insertion of the adsorbate molecules using GCMC particle addition moves up to the predefined concentration. After the particle insertion the system was equilibrated using NVT Monte Carlo (100 000 single particle moves), followed by 100 000 MD steps. After equilibration a production run with 4.8×10^6 MD steps was performed. Throughout the MD simulation the temperature was held constant with a Nosé-Hoover thermostat. The time steps used were 4.38 fs for CH_4, 10.28 fs for CF_4, 2.19 fs for He, 4.93 fs for Ne, 6.93 fs for Ar, 12.57 fs for Xe, and 13.25 fs for SF_6. During the production run the molecular coordinates were saved every 20 time steps. The *x*, *y*, and *z* components of the self-and corrected diffusivity were then calculated from the saved trajectories using a so-called order N algorithm.[33] Since the corrected diffusivity is a collective property (see eq 11) it is not possible to get an accurate result from just one trajectory. Thus for all our simulations we have restricted our runs to 4.8×10^6 time steps but used 20 independent trajectories for each set of conditions. The average diffusivities and their uncertainties were then calculated from the results of the 20 independent trajectories.

In any MD calculation of diffusivities, it is important to verify that well converged results are obtained. This fact is highlighted by a recent paper by Kar and Chakravarty on diffusional anisotropy in silicalite.[40] In that paper, MD simulations were performed in the NVE ensemble for several of the same species we have considered. These simulations used a simulation volume of $1 \times 1 \times 2$ unit cells for all studied concentrations and averaged data over only one simulation run. This very small sample size compromises the quality of the results reported, particularly at low loadings. For example, Kar and Chakravarty report that the orientationally averaged self diffusivity for CH_4 at a loading of 4 molecules/unit cell and $T = 298$ K is 0.4×10^{-4} cm^2/s. This value is more than 30% lower than the value we find in our calculations, which use the same intermolecular potentials. Unlike the results of Kar and Chakravarty, our results are in quantitative agreement with previous simulations of this model.[41] This observation is illustrated in Figure 3, which shows the orientationally averaged self diffusivity of CH_4 in silicalite at 298 K from our calculations compared to those of multiple groups who have previously simulated the same atomistic model. One quantity that appears to be particularly inaccurate in the work of Kar and Chakravarty is the *z*-component of the self diffusivity. This is the slowest of the three components of D_s in silicalite, so it is the most challenging to compute accurately. Unfortunately, many of the conclusions in ref 40 rely on comparing the various components of D_s. Our more fully resolved calculations strongly indicate that these conclusions are largely incorrect due to lack of convergence in ref 40. We return to this point below when we discuss the anisotropy of self diffusion in silicalite. To indicate the quality of convergence in our calculations, we show in Figure 4 the components and orientational average of D_s for CH_4 in silicalite at 8 molecules/unit cell. As indicated above, our data comes from 20 independent 21.0 ns MD simulations in a $2 \times 2 \times 2$ unit cell simulation volume. Our data is analyzed by breaking each trajectory into a set of independent sub-trajectories, each with a fixed time span. Figure 4 shows the observed results for this set of simulations as the length of the time spans is varied. As expected, the error bars increase slightly in size as longer time spans are used because the data is averaged over fewer sub-trajectories in this case. Apart from this effect, each individual component and, as a result, the orientationally averaged value of D_s is consistent across the range of time spans shown in Figure 4. We have obtained analogous results for our calculations of corrected diffusivities.

As noted in eq 5, the self, corrected, and transport diffusivities are equal at the limit of vanishing concentration. We have computed this limiting diffusivity, $D(0)$, for each of the gas species we have simulated. To do this, we performed EMD simulations as described above with 5 molecules per unit cell after setting the adsorbate−adsorbate interaction energy to zero. The results of these calculations are listed in Table 2. The diffusivities of the various species vary by more than 2 orders of magnitude and, as expected, decrease as the molecular weight of the adsorbed species increases.

III. Self Diffusivities

The orientationally averaged self diffusivities for the seven species we have simulated are shown as a function of pore

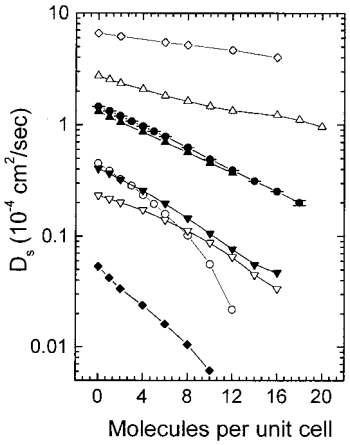

Figure 5. Orientationally averaged self diffusivities in silicalite at 298 K. The adsorbate species are indicated in the same way as in Figure 1.

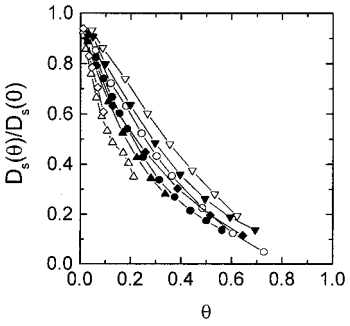

Figure 6. The same data as in Figure 5, but plotted as a normalized diffusivity versus fractional loading as described in the text.

loading in Figure 5. As with all the results presented in this paper, these data correspond to adsorption at 298 K. The uncertainties shown in Figure 5 for CH_4 are typical of those observed for the other six species. The trends evident in Figure 5 are well-known from previous studies. For each species, D_s decreases as the pore loading is increased due mainly to steric interactions between adsorbates. As noted above, the magnitude of the diffusivities decreases as the adsorbate mass is increased. It is interesting to note that data for most of the species we have considered is well described by a straight line in the log−linear coordinates used in Figure 5.

The orientationally averaged self diffusivities are replotted in dimensionless form in Figure 6. In this figure, each diffusivity is normalized by the zero loading diffusivity for the species being considered and the loading is normalized by the saturation loading. Figure 6 shows that each species can be described with eq 7, although the correlation function, $f(\theta)$, is different for each species. Loosely speaking, the more strongly the function f deviates from unity, the more strongly the motion of individual molecules is dependent on their recent history. For the species we considered, the two lightest, He and Ne, show the strongest correlations in this sense.

The use of orientationally averaged diffusivities in Figures 5 and 6 masks the fact that diffusion in silicalite is anisotropic. One simple measure of diffusional anisotropy in this material is the ratio of diffusivities in the x and y directions, $D_{s,x}/D_{s,y}$. This ratio is plotted as a function of fractional loading for each species in Figure 7a. Since diffusion along the straight channels (y direction) is faster than diffusion along the zigzag channels (x direction), $D_{s,x}/D_{s,y} < 1$ in all cases. The largest species we simulated, SF_6, shows the most extreme anisotropy. In all cases, diffusion initially becomes slightly less anisotropic as the loading is increased from zero. For the species that were simulated at

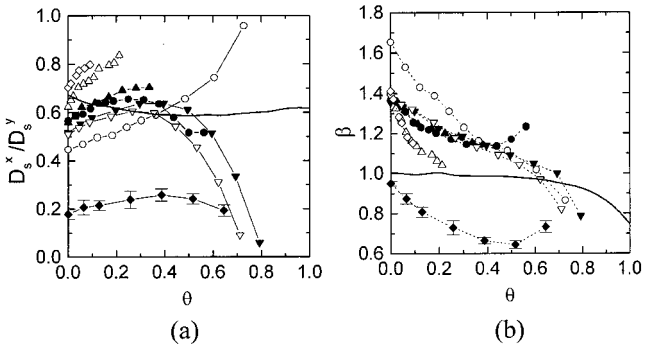

Figure 7. (a) The ratio of the x and y components of self diffusivity in silicalite at 298 K. (b) $\beta = c^2/D_{s,z}\,(a^2/D_{s,x} + b^2/D_{s,y})^{-1}$ as a function of fractional loading for the same systems. In each case, the adsorbate species are indicated in the same way as Figure 1. The solid curves show the results of the LG model of CH_4 due to Paschek and Krishna.[42]

high loadings, the anisotropy increases then decreases as the loading is further increased, except CF_4, which continues to become less anisotropic. The solid curve in Figure 7a is the result from the LG model of CH_4 in silicalite by Paschek and Krishna.[42] By using slightly different hopping rates for diffusion moves from sites in different channel types, this model represents the orientationally averaged self diffusivity very well (assuming a saturation loading of 24 molecules/unit cell).[42] From Figure 7a we see that this LG model does a reasonable job of capturing the anisotropy of self diffusion, although the detailed trends in the anisotropy are not reproduced.

A second quantity characterizing diffusional anisotropy in silicalite was proposed by Kärger, who noted that diffusion in the x, y, and z directions are not all independent because of silicalite's pore connectivity.[43] He showed analytically that a single adsorbate that hops in an uncorrelated manner on a lattice of sites with silicalite's topology satisfies $(c^2/D_{s,z}) = (a^2/D_{s,x}) + (b^2/D_{s,y})$, regardless of the ratio $D_{s,x}/D_{s,y}$.[43] To examine the validity of this expression, it is natural to define

$$\beta = \frac{c^2/D_{s,z}}{(a^2/D_{s,x} + b^2/D_{s,y})} \tag{12}$$

For any molecule that diffuses through silicalite in a completely Markovian manner, $\beta = 1$. Although Kärger's expression only strictly applies to a single adsorbate hopping on a lattice, it is typically found to be approximately correct for a broad range of loadings in LG models. An example of this result is shown as a solid curve in Figure 7b, which gives β as a function of coverage for the LG model of CH_4 in silicalite by Paschek and Krishna.[42] The values of β determined from our atomistic simulations are also shown in Figure 7b. It is clear that the atomistic results are qualitatively different from those predicted by LG models. Specifically, $\beta > 1$ at zero loading for all of the species we have examined except SF_6. As pointed out by Kar and Chakravarty, values of $\beta > 1$ indicate that individual molecules prefer to continue their motion in the channel they are initially located in rather than move into the opposite channel type.[40] The only species that does not follow this pattern is SF_6, which, since $\beta < 1$, prefers to switch channel types when it moves through a channel intersection. We can at present offer no satisfactory microscopic mechanism for the observation that only the largest molecule we have simulated shows this tendency to switch channel types at channel intersections.

It is important for us to compare our results regarding diffusional anisotropy to those presented recently by Kar and Chakravarty.[40] The results reported in ref 40 were based on

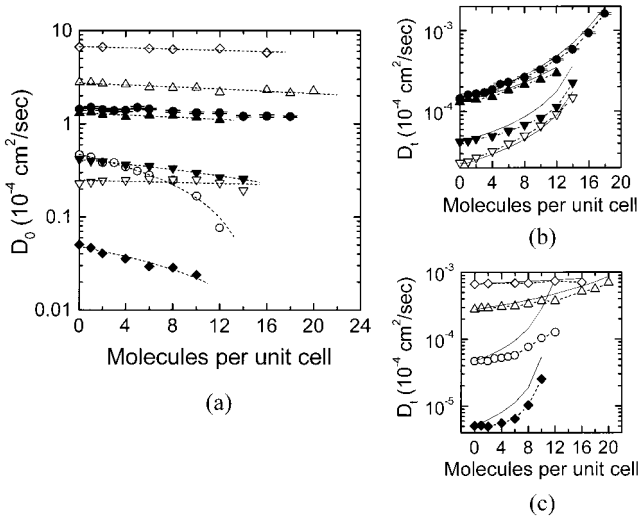

Figure 8. (a) The corrected diffusivity, D_0, of various adsorbates in silicalite at 298 K. (b) and (c) The transport diffusivity, D_t, of the same adsorbates. In each plot, the adsorbate species are indicated in the same way as Figure 1. Dotted curves are to guide the eye. The solid curves in (b) and (c) are the predictions of the Darken approximation, eq 6.

considerably shorter MD runs than those we have used. As we noted above, it is not clear that diffusivities computed by Kar and Chakravarty are accurate. The value of $D_{s,x}/D_{s,y}$ we observed are in reasonable agreement with those in ref 40 at loadings above 8 molecules per unit cell. At lower loadings, there is a considerable discrepancy between our results and those of ref 40. We believe that this is due to the poor convergence of Kar and Chakravarty's simulations, whose method was particularly prone to inaccuracy at low loadings. This is particularly evident in the results reported in ref 40 for $D_{s,z}$, the slowest component of the self diffusivity. An unfortunate consequence of this is that the values of β reported by Kar and Chakravarty are quantitatively and qualitatively incorrect. They give values of β that are almost without exception smaller than 1, in contrast to our data in Figure 7b. We reiterate that our results are based on much larger simulations than those of ref 40 and for the reasons outlined in section II we believe our results exhibit much better convergence properties. As a result, the values of β shown in Figure 7b should be thought of as replacing those reported in ref 40.

IV. Corrected and Transport Diffusivities

We have used the equilibrium MD methods described above to calculate the corrected diffusivity, D_0, as a function of loading for each of the seven species at 298 K. The resulting diffusivities are summarized in Figure 8a. The error bars shown on the CH_4 data in Figure 8a are indicative of the uncertainties in all seven species. For most of the species, the corrected diffusivity shows a much weaker dependence on loading than the self diffusivity (cf. Figure 5), although both diffusivities decrease with increased loading in all cases. Since the corrected and self diffusivities are identical in the limit of zero loading, the ordering of the species in this limit is the same in Figure 8a and Figure 5.

As shown in eq 4, the transport and corrected diffusivities are closely related. To calculate the thermodynamic correction factor in eq 4, we fitted the adsorption isotherm for each species using a dual-site Langmuir isotherm:

$$n = \frac{A_1 \cdot P}{B_1 + P} + \frac{A_2 \cdot P}{B_2 + P} \qquad (13)$$

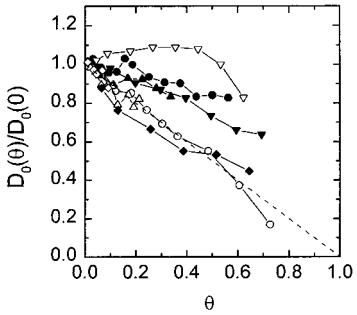

Figure 9. The same as Figure 6 but using corrected diffusivities instead of self diffusivities. The dashed line shows the lattice gas result.

The resulting transport diffusivities are shown as symbols in Figure 8b and 8c. For each of the seven species we simulated, D_t increases as a function of pore loading. As mentioned in our earlier work,[9] the values of D_t we observe for CH_4 are entirely consistent with the earlier results of Maginn et al.[17] based on NEMD simulations.

The results in Figure 8 are useful for examining the validity of the two most common approximations used for the transport diffusivity, eqs 6 and 9. We look first at the so-called Darken approximation, eq 6, which assumes that the corrected diffusivity, D_0, is independent of the pore loading. It is clear from Figure 8a that this assumption is not entirely correct, although it is a reasonable approximation for several of the species we simulated. The transport diffusivities predicted using eq 6 are shown in Figures 8b and 8c as solid curves. In calculating these curves, we used the same thermodynamic correction factors determined from eq 13. In every case, the Darken approximation overestimates the transport diffusivity at nonzero pore loadings. Since the true corrected diffusivities decrease with loading, the discrepancy between the actual transport diffusivity and that predicted by the Darken approximation increases as the pore loading is increased. As noted in previous work, approximating the corrected diffusivity as a constant independent of pore loading is quite accurate for CH_4 in silicalite. The results in Figure 8 indicate that the same statement also applies to Ar and Ne. In contrast, the actual diffusivities for CF_4 and SF_6 deviate strongly from this approximation. The behavior of CF_4 was reported by us previously,[9] and it remains the most severe departure from the Darken approximation we have observed in silicalite. The inaccuracy of the Darken approximation for these species naturally has significant consequences if the results of this approximation are used in quantitative calculations. One example of this is in the modeling of zeolite membranes, where the Darken approximation is often invoked to describe single-component transport. We have shown that if the Darken approximation is used in this manner, the ideal selectivity of CH_4 over CF_4 through silicalite membranes is greatly underpredicted relative to the correct result.[36]

The second common approximation for the corrected and transport diffusivities is the one arising from LG models of molecular diffusion, eqs 8 and 9. The observation that the measured transport diffusivities of every species increase with loading (Figure 8b and 8c) immediately indicates that these LG approximations are not quantitatively accurate. We have plotted the corrected diffusivities as a function of fractional loading in Figure 9. One caveat in interpreting Figure 9 is that because of the method we used to determine the saturation loadings (see above), the adsorption isotherms cannot accurately be described as Langmuir isotherms with saturation loading n_{sat} molecules/unit cell, even though this isotherm is the one that arises from simple LG models. Aside from this complication, the results in

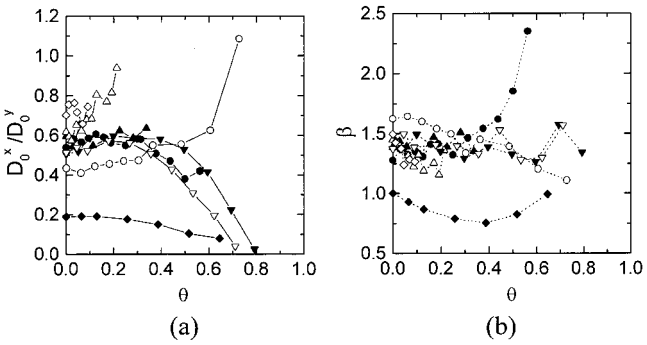

Figure 10. The same as Figure 7 but using components of the corrected diffusivities instead of self diffusivities.

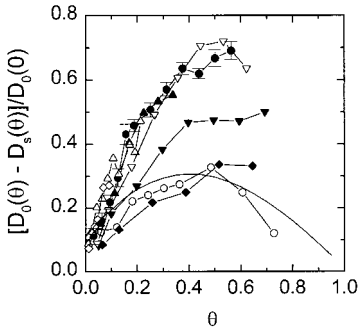

Figure 11. Contributions of interparticle correlations to the corrected diffusivity normalized by the zero loading diffusivity shown as a function of the loading. The different species are indicated in the same way as Figure 1. The solid curve shows the LG result due to Paschek & Krishna.[42]

Figure 9 can be directly compared to the LG prediction that $D_0^{LG}(\theta)/D(0) = (1 - \theta)$.The species that gave the worst agreement with the Darken approximation, CF_4 and SF_6, are in reasonable agreement with the LG prediction. Of course, the species that yielded reasonable agreement with the Darken approximation such as CH_4 show substantial deviations from the LG prediction.

The directional anisotropy of the corrected diffusivities can be assessed using the same quantities we described above for self diffusivities. The results of this analysis are summarized in Figure 10. Although there is more scatter in the corrected diffusivities than in the self diffusivities, the main trends observed in the anisotropy of the latter quantity are also seen in the corrected diffusivities.

The results presented in this section are the largest collection of corrected and transport diffusivities determined from atomistic simulations of molecular diffusion in zeolites to date. Perhaps the most important general conclusion that can be drawn from these results is that neither the corrected nor the transport diffusivity is in general independent of pore loading. For the seven species we have examined, the Darken approximation, eq 6, systematically overestimates the transport diffusivity, while the LG approximation, eq 9, systematically underestimates the transport diffusivity. Each of these approximations is quite accurate for one or two of the seven species we simulated. In the next section we discuss the root causes of this range of observed behaviors.

V. Discussion

Understanding the macroscopic mass transfer of adsorbed species inside zeolite pores is fundamental to most practical applications of these materials. These phenomena can be characterized using either the transport diffusivity, D_t, or the corrected diffusivity, D_0, as described in our introduction. We have used equilibrium MD and GCMC simulations to directly determine D_t and D_0 for atomistic models of seven light gases adsorbed in silicalite at 298 K. These results provide a useful basis for examining the accuracy of common approximations to these two diffusivities.

Before discussing our results quantitatively, we reiterate our main qualitative conclusions. For every species we examined, the corrected diffusivity decreases as a function of pore loading while the transport diffusivity increases. Neither the Darken approximation of a constant corrected diffusivity or the LG approximation of a constant transport diffusivity is in general correct. However, there is at least one species in the set we examined that is well approximated by each approximation. Finally, we note that the ability of a LG model to accurately reproduce the loading dependence of an adsorbate's self diffusivity does not imply that the same model accurately captures the corrected and transport diffusivities of that adsorbate. The LG model of Paschek and Krishna for CH_4 in silicalite[42] is a specific example of the last observation.

To discuss our results in more detail, it is useful to note that the corrected diffusivity can be explicitly related to the self diffusivity by[2]

$$D_0 = D_s + \frac{1}{3N}\sum_{i=1}^{N}\sum_{j=1}^{N}{}' \int_0^\infty \langle \mathbf{v}_i(0)\,\mathbf{v}_j(t)\rangle \, \mathrm{d}t \qquad (14)$$

where the second summation on the right-hand side excludes terms with $i=j$. That is, the corrected diffusivity is equal to the self diffusivity plus a term that arises solely due to correlated motions in pairs of adsorbates. These inter-adsorbate correlations can appear in several distinct ways. First, the motion of one adsorbate may create a vacancy into which a nearby adsorbate moves a short time later. This type of correlated motion occurs even in LG models where adsorbates hop in an entirely Markovian manner. It is these correlations that cause the differences between self and corrected diffusivities in LG models,[12,13,42] which are typically small. A second type of correlated motion that cannot occur in LG models but is present in atomistic descriptions is the transfer of momentum during collisions between neighboring adsorbates. A third type of correlated motion can arise if weakly bound clusters of adsorbates move in a concerted way through a pore. This type of motion has been shown to have significant effects for several species that perform single-file diffusion in the pores of $AlPO_4$-5,[7,44,45] although the generality of this phenomenon in more complex pore structures is undetermined.

The ability of simple LG models to describe adsorbate diffusion accurately depends to a large extent on the importance of the second and third contribution to correlated particle motion listed above. The contribution of interparticle correlations to the corrected diffusivity in our simulations can be seen by plotting $(D_0(\theta) - D_s(\theta))/D(0)$. This quantity is zero in the limit of zero loading because in this limit there are no interparticle correlations. This quantity is plotted for the seven species we have simulated in Figure 11. In all cases except CF_4 and SF_6, the contribution to diffusion from interparticle correlations is substantially larger than that seen in LG models.

It is helpful to ask why the diffusion of CF_4 and SF_6 in silicalite includes relatively small contributions from inter-adsorbate correlations. One simple possibility is that diffusion of a single molecule of these species is a highly activated process. In this case, the corrugation of the adsorbate−zeolite

potential energy surface could be so large that adsorbate−adsorbate interactions are negligible. Said differently, CF_4 and SF_6 may show only small interparticle correlations because their motion is very similar to that assumed in lattice models. This scenario can be quantified by the ratio of the activation energy for an isolated molecule diffusing, E_{ads}, to the adsorbate−adsorbate interaction energy, ϵ_{aa}. To determine E_{ads}, we computed the orientationally averaged $D(0)$ for CF_4, SF_6, and CH_4 at 298, 373, and 473 K, then fitted these results to the usual Arrhenius form. This gives the apparent activation energy for self diffusion of an isolated adsorbate as 4.25 kJ/mol for CH_4,[36] 4.43 kJ/mol for CF_4, and 7.44 kJ/mol for SF_6. The ratio ϵ_{aa}/E_{ads} is therefore 3.5, 4.0, and 4.0 for CH_4, CF_4, and SF_6, respectively. Crucially, both the absolute activation energy and the ratio of the activation energy to the adsorbate−adsorbate interaction strength are very similar for CH_4, which shows substantial interparticle correlations, and CF_4, which shows very little effect from interparticle correlations. Although the activation energy for SF_6 diffusion is somewhat larger than the other two species, the relative size of the adsorbate−adsorbate interactions is very similar to the other two examples. From these results, we can see that it is not correct to say that the difference in interparticle correlations between CF_4 and CH_4 is because CF_4 is "lattice-like" and CH_4 is more "fluid-like".

The discussion above suggests that an important factor in determining the amount of interparticle correlations is the efficiency of momentum transfer between pairs of particles during adsorbate−adsorbate collisions. This idea can be considered by describing the chain of events that follows a collision between two adsorbates. The interparticle velocity autocorrelation function in eq 14 will give a positive contribution to the corrected diffusivity if momentum from one particle is largely transferred to the other particle during a collision. For the purposes of our discussion, imagine that a collision between particles 1 and 2 occurs at $t = 0$, transferring momentum from particle 1 to particle 2. If the particles are large compared to the confining pore, the interval between this collision and a collision between particle 2 and the pore wall is typically very short. These wall collisions will rapidly decorrelate the momentum the second particle acquired from particle 1. On the other hand, if the particles are small relative to the confining pore, there is a much greater probability that the new momentum of particle 2 does not lead immediately to a collision with a wall and subsequent decorrelation of that particle's motion. That is, the volume of phase space over which particle 2 may travel in a correlated manner is much greater for smaller adsorbates than larger adsorbates. This explanation is not quantitative, but it captures the qualitative result from our data that the largest adsorbates are the ones that show small interparticle correlations.

Although our discussion above distinguished between small and large adsorbates by using the pore size, it is more accurate to think about the transfer of momentum during particle collisions with respect to the topology of the potential energy surface. In a cylindrical pore, for example, an adsorbate that is small relative to the pore diameter will typically be confined in an annulus inside the pore perimeter. In the limit of a very large pore, the confining surface of this annulus is two-dimensional.[38] In the same cylindrical pore, adsorbates similar in size to the pore are typically confined to a narrow cylindrical volume in the center of the pore. This volume is essentially one-dimensional.[38] This reduction in dimensionality may reduce the opportunities for correlated transfer of momentum between adsorbates in the latter system relative to the case with small adsorbates.

This discussion indicates that the precise nature of the interparticle correlation contributions to the corrected diffusivity will depend on the detailed structure of the potential energy surface upon which the adsorbates move. There does not seem to be any a priori reason to expect that the interparticle correlations will exactly offset the changes in the self diffusivity with loading, leading to a corrected diffusivity that is loading independent as predicted by the Darken approximation. In other words, there is no reason to expect that the Darken approximation is quantitatively accurate for any system of adsorbates and adsorbent. This is entirely consistent with the spirit in which this approximation was originally proposed, namely a method that was motivated largely by the need for simplicity.[4] In this context, the level of agreement between the Darken approximation and the diffusion of CH_4 in silicalite is all the more remarkable.

It is interesting to speculate how the ideas emerging from the discussion above may apply to several aspects of molecular transport in nanoporous materials. First, we consider the diffusion of molecules similar to those we have studied diffusing in mesoporous materials such as MCM-41. In general, we expect that the open nature of the pores in these materials will offer a favorable environment for the transfer of momentum between adsorbates. At the same time, the steric effects that lead to the rapid decrease in self diffusivities as a function of loading in micropores also exist in the mesoporous materials. This suggests that in mesoporous materials, self diffusivities will decrease rapidly with pore loading, but corrected diffusivities will be a much weaker function of pore loading. It is interesting to note in this context that recent simulations by Malek and Coppens of dilute gases diffusing in fractally rough pores have indicated a similar result for self and transport diffusivities as a function of the pore roughness.[46]

A second situation we can consider is the diffusion of extended molecules such as long chain hydrocarbons in zeolite micropores. Again, steric effects indicate that molecular self diffusivities will decrease strongly as a function of pore loading. In the case of extended molecules, the interparticle velocity autocorrelations appearing in eq 14 refer to the motion of the centers of mass of molecules. The existence of many internal degrees of freedom in a diffusing molecule offer many channels through which momentum transferred by intermolecular collisions can rapidly become decorrelated. This argument indicates that the contributions of interparticle correlations to the corrected diffusivity will decrease quite strongly with the number of internal degrees of freedom in the molecule being considered. In this case, the corrected and self diffusivities have essentially the same dependence on pore loading. This observation has important implications for experimental comparisons between self and transport diffusivities, since it implies that the Darken approximation will generally substantially overestimate the transport diffusivities of extended molecules in zeolite micropores.

A final situation we can consider is the implications of our results for multicomponent diffusion. One convenient way to formulate a macroscopic description of mass transport in a system containing n adsorbed species is using the Onsager expression[2,47,48]

$$\vec{\mathbf{J}}_i = -\sum_{i=1}^{n} L_{ij} \nabla \mu_j \tag{15}$$

This formulation is of course formally equivalent to other possible formulations such as the Maxwell-Stefan method.[49] In

the Onsager formulation, the diagonal elements of the Onsager coefficients can be written as[2]

$$L_{ii} = \frac{1}{3VkT}\sum_{j=1}^{N_i}\int_0^\infty \langle \mathbf{v}_j(0)\,\mathbf{v}_j(t)\rangle\,\mathrm{d}t + \frac{1}{3VkT}\sum_{j=1}^{N_i}\sum_{k=1}^{N_i}{}'\int_0^\infty \langle \mathbf{v}_j(0)\,\mathbf{v}_k(t)\rangle\,\mathrm{d}t \quad (16)$$

where there are N_i molecules of species i. The similarity between this expression and eq 14 is evident. The cross-species interactions are described by the symmetric off-diagonal phenomenological coefficients, $L_{ij} = L_{ji}$ $(i \neq j)$. These coefficients can be expressed in terms of velocity autocorrelation functions as[2]

$$L_{ij} = \frac{1}{3VkT}\sum_{k=1}^{N_i}\sum_{m=1}^{N_j}\int_0^\infty \langle \mathbf{v}_k(0)\,\mathbf{v}_m(t)\rangle\,\mathrm{d}t,\ (i \neq j) \quad (17)$$

where the first (second) sum is over molecules of species i (j). Comparison of this expression with eq 14 shows that the cross-species interactions are completely analogous to the interparticle correlations that arise in the single-component corrected diffusivity except that they are restricted to pairs of particle of different species. This observation allows us to immediately make several comments regarding the importance of inter-species interactions in multicomponent transport. If two species which both show poor intra-species momentum transfer are present in the same adsorbent, our qualitative arguments above indicate that the inter-species correlations in this case will also be small. Hence, the off-diagonal Onsager coefficients are likely to be negligible in this case and the diagonal elements are dominated by the self diffusion in the multicomponent system. In the other extreme, if both species show favorable intra-species correlations, then the inter-species correlations will not be negligible. In the intermediate case where one species has good inter-species correlations but the other does not, it seems likely that the cross-species interactions will not always be small. In this case, one can imagine that transfer of momentum from the large species to the small species might take place in a relatively correlated way, although the reverse process might not be so efficient. Although these ideas are somewhat speculative, they can be directly tested by extending the types of simulations we have discussed in this paper to simulations of binary mixtures. We are currently performing simulations of this type and will report on the outcome of this work in the future.

Acknowledgment. This work was supported by a National Science Foundation CAREER award (CTS-9983647) and by Air Products and Chemicals Inc. A.I.S. gratefully acknowledges a scholarship from the Alexander S. Onassis Public Benefit Foundation. D.S.S. is an Alfred P. Sloan fellow. Computing resources were provided by the Pittsburgh Supercomputer Center and through a computer cluster in our department supported by the NSF (CTS-0094407) and Intel.

References and Notes

(1) Kärger, J.; Ruthven, D. *Diffusion in Zeolites and Other Microporous Materials*; John Wiley & Sons: New York, 1992.
(2) Theodorou, D. N.; Snurr, R. Q.; Bell, A. T. Molecular Dynamics and diffusion in microporous materials. In *Comprehensive Supramolecular Chemistry*; Alberti, G., Bein, T., Eds.; Pergamon Press: New York, 1996; Vol. 7, pp 507−548.
(3) Keil, F. J.; Krishna, R.; Coppens, M. O. *Rev. Chem. Eng.* **2000**, *16*, 71−197.
(4) Reyes, S. C.; Sinfelt, J. H.; DeMartin, G. J. *J. Phys. Chem. B* **2000**, *104*, 5750−5761.
(5) Auerbach, S. M. *Int. Rev. Phys. Chem.* **2000**, *19*, 155−198.
(6) Uebing, C.; Gomer, R. *J. Chem. Phys.* **1994**, *100*, 7759−7766.
(7) Sholl, D. S. *Ind. Eng. Chem. Res.* **2000**, *39*, 3737−3746.
(8) Mak, C. H.; Andersen, H. C.; George, S. M. *J. Chem. Phys.* **1988**, *88*, 4052−4061.
(9) Skoulidas, A. I.; Sholl, D. S. *J. Phys. Chem. B* **2001**, *105*, 3151−3154.
(10) Darken, L. S. *Trans. AIME* **1948**, *175*, 184.
(11) Skoulidas, A.; Sholl, D. In preparation.
(12) Trout, B. L.; Chakraborty, A. K.; Bell, A. T. *Chem. Eng. Sci.* **1997**, *52*, 2265−2276.
(13) Coppens, M. O.; Bell, A. T.; Chakraborty, A. K. *Chem. Eng. Sci.* **1999**, *54*, 3455−3463.
(14) Chen, L. G.; Falcioni, M.; Deem, M. W. *J. Phys. Chem. B* **2000**, *104*, 6033−6039.
(15) Paschek, D.; Krishna, R. *Phys. Chem. Chem. Phys.* **2000**, *2*, 2389−2394.
(16) Paschek, D.; Krishna, R. *Chem. Phys. Lett.* **2001**, *333*, 278−284.
(17) Maginn, E. J.; Bell, A. T.; Theodorou, D. N. *J. Phys. Chem.* **1993**, *97*, 4173−4181.
(18) Snurr, R. Q.; Kärger, J. *J. Phys. Chem. B* **1997**, *101*, 6469−6473.
(19) Goodbody, S. J.; Watanabe, K.; MacGowan, D.; Walton, J. P. R. B.; Quirke, N. *J. Chem. Soc., Faraday Trans.* **1991**, *87*, 1951−1958.
(20) Paschek, D.; Krishna, R. *Phys. Chem. Chem. Phys.* **2001**, *3*, 3185−3191.
(21) Heuchel, M.; Snurr, R. Q.; Buss, E. *Langmuir* **1997**, *13*, 6795−6804.
(22) Reid, R. C.; Prausnitz, J. M.; Poling, B. E. *Properties of Gases and Liquids*; McGraw-Hill: New York, 1987.
(23) Clark, L. A.; Gupta, A.; Snurr, R. Q. *J. Phys. Chem. B* **1998**, *102*, 6720−2731.
(24) Hirschfelder, J. O.; Curtiss, C. F.; Bird, R. B. *Molecular Theory of Gases and Liquids*; Wiley & Sons: New York, 1954.
(25) June, R. L.; Bell, A. T.; Theodorou, D. N. *J. Phys. Chem.* **1991**, *95*, 8866−8878.
(26) Pickett, S. D.; Nowak, A. K.; Thomas, J. M.; Peterson, B. K.; Swift, J. F. P.; Cheetham, A. K.; den Ouden, C. J. J.; Smit, B.; Post, M. F. M. *J. Phys. Chem.* **1990**, *94*, 1233−1236.
(27) Chakravarty, C. *J. Phys. Chem. B* **1997**, *101*, 1878−1883.
(28) Maitland, G. C.; Rigby, M.; Smith, E. B.; Wakeham, W. A. *Intermolecular Forces: Their Origin and Determination*; Clarendon Press: Oxford, 1981.
(29) Olson, D. H.; Kokotailo, G. T.; Lawton, S. L.; Meier, W. M. *J. Phys. Chem.* **1981**, *85*, 2238−2243.
(30) Demontis, P.; Fois, E. S.; Suffritti, G. B.; Quartieri, S. *J. Phys. Chem.* **1990**, *94*, 4329−4334.
(31) June, R. L.; Bell, A. T.; Theodorou, D. N. *J. Phys. Chem.* **1990**, *94*, 8232−8240.
(32) Schultz, M. *Spline Analysis*; Prentice Hall: Englewood Cliffs: NJ, 1973.
(33) Frenkel, D.; Smit, B. *Understanding Molecular Simulation: From Algorithms to Applications*; Academic Press: London, 1996.
(34) Doulsin, D. R.; Harrison, R. H.; Moore, R. T. *J. Phys. Chem.* **1967**, *71*, 3477−3488.
(35) Dymond, J. H.; Smith, E. B. *The Virial Coefficients of Gases—A Critical Compilation*; Clarendon Press: Oxford, 1969.
(36) Bowen, T. C.; Falconer, J. L.; Skoulidas, A. I.; Sholl, D. D. *Ind. Eng. Chem. Res.* **2002**, *41*, 1641−1650.
(37) Dunne, J. A.; Mariwals, R.; Rao, M.; Sircar, S.; Gorte, R. J.; Myers, A. L. *Langmuir* **1996**, *12*, 5888−5895.
(38) Challa, S. R.; Sholl, D. S.; Johnson, J. K. *Phys. Rev. B* **2001**, *63*, No. 245419.
(39) Snurr, R. Q.; Bell, A. T.; Theodorou, D. N. *J. Phys. Chem.* **1993**, *97*, 13742−13752.
(40) Kar, S.; Chakravarty, C. *J. Phys. Chem. A* **2001**, *105*, 5785−5793.
(41) Jost, S.; Bär, N.; Fritzsche, S.; Haberlandt, R.; Kärger, J. *J. Phys. Chem. B* **1998**, *102*, 6375−6381.
(42) Paschek, D.; Krishna, R. *Langmuir* **2001**, *17*, 247−254.
(43) Kärger, J. *J. Phys. Chem.* **1991**, *95*, 5558−5560.
(44) Sholl, D. S. *Chem. Phys. Lett.* **1999**, *305*, 269−275.
(45) Sholl, D. S.; Lee, C. K. *J. Chem. Phys.* **2000**, *112*, 817−824.
(46) Malek, K.; Coppens, M.-O. *Phys. Rev. Lett.* **2001**, *87*, 125505.
(47) Sanborn, M. J.; Snurr, R. Q. *Sep. Purif. Technol.* **2000**, *20*, 1−13.
(48) Sanborn, M. J.; Snurr, R. Q. *AIChE J.* **2001**, *47*, 2032−2041.
(49) Krishna, R.; Vandenbroeke, L. J. P. *Chem. Eng. J. Biochem. Eng.* **1995**, *57*, 155−162.